Compressive sensing algorithm for 2D reconstruction of THz digital holography

Yunda Li (李运达), Qi Li (李 琦), Jiaqi Hu (胡佳琦), and Yongpeng Zhao (赵永蓬)

National Key Laboratory of Science and Technology on Tunable Laser, Harbin Institute of Technology, Harbin 150080, China

Corresponding author: liqi2013@hit.edu.cn

Received April 3, 2014; accepted July 16, 2014; posted online January 26, 2015

We present an improved compressive sensing algorithm with negative transformation and piecewise-nonlinear transformation. The reconstruction characteristics of the improved algorithm are studied by conducting numerical analysis research. Watch gear and handwritten character are used in the experiments. The results validate the application value of the improved algorithm in improving 2D reconstructed image quality in terahertz (THz) Gabor inline digital holography.

OCIS codes: 110.0110, 110.6795, 110.3000.

doi: 10.3788/COL201513.S11101.

Terahertz (THz) electromagnetic radiation can penetrate some nonmetallic and nonpolar materials. THz imaging can make up the defect of imaging opaque samples in visible light domain. Digital holography is a new technology for extracting full information of the original object. There have been increasing research reports on THz digital holographic imaging[1–7]. Major reconstruction algorithms in THz Gabor inline holography have included angular spectrum algorithm and phase retrieval[1,7].

As Gabor inline holography satisfies a sufficient condition called the restricted isometry property (RIP), during the past few years, compressive sensing (CS)[8] algorithm has been used to reconstruct a single hologram in Gabor inline digital holography[9–11]. CS searches for the sparsest solution via an optimization procedure. In 2009, Denis *et al.* have experimentally validated that the 2D visible light images obtained with their iterative algorithm are free from the artifacts of the conventional methods, such as out-of-focus objects and twin images[12]. We have used CS for THz tomography, and a modified reconstruction algorithm has been proposed by coupling CS algorithm with negative transform, apodization, and piecewise-nonlinear transformation function[13]. To the best of our knowledge, there are no relevant detailed research reports on improving 2D reconstructed image quality in THz Gabor inline digital holography.

In this letter, CS algorithm with negative transformation and piecewise-nonlinear transformation are used to reconstruct images. Numerical analysis and experimental studies are conducted.

The schematic diagram of continuous-wave (CW) THz Gabor inline digital holographic imaging system is shown in Fig. 1. After THz wave illuminated a sample, the diffraction wave of the sample interferes with the transmitting THz wave on the photosurface, and the interference pattern is recorded as the hologram. The reconstructed images are obtained with reconstruction algorithms.

The amplitude of the reference plane wave is assumed to be 1 without loss of generality, and the plane wave illuminates perpendicularly. It is assumed that $o(x_0, y_0, z_0)$ is the scattering amplitude of a 3D object, the sample spacings along the x- and y-axes are $\Delta_x = \Delta_y = \Delta$ and the sampling pitch is Δ_z in the z-axis. The number of pixels along the x- and y-axes dimension is N_x and the number of 2D discrete planes along the z-axis is N_z. Based on the Rayleigh–Sommerfeld diffraction integral function, the discrete model of the scattered field in the hologram plane can be expressed as

$$U_{\mathrm{H}}(m_{\mathrm{H}}, n_{\mathrm{H}}) = \sum_{l_0=1}^{N_z} \sum_{m_0=1}^{N_x} \sum_{n_0=1}^{N_x} \Big[o_{l_0}(m_0\Delta, n_0\Delta, l_0\Delta_z) \times h_{l_0} ((m_{\mathrm{H}} - m_0)\Delta, (n_{\mathrm{H}} - n_0)\Delta) \Big], \quad (1)$$

where m_{H} and n_{H} represent the pixel position in the hologram plane, o_{l_0} is the amplitude distribution of a certain 2D plane of o. h_{l_0} is the systematic impulse response function, which can be expressed as

$$h_{l_0}(m,n) = \frac{1}{\mathrm{j}\lambda l_0 \Delta_z \left[1 + (m\Delta/l_0\Delta_z)^2 + (n\Delta/l_0\Delta_z)^2\right]} \times \exp\left[\mathrm{j}\frac{2\pi\sqrt{(l_0\Delta_z)^2 + (m\Delta)^2 + (n\Delta)^2}}{\lambda}\right]. \quad (2)$$

The recorded hologram I can be discretely expressed as[6,7]

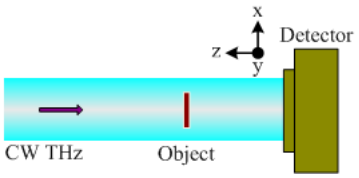

Fig. 1. Schematic diagram of CW THz Gabor inline digital holographic imaging system.

$$I(m_{\mathrm{H}},n_{\mathrm{H}}) = |\,1+U_{\mathrm{H}}(m_{\mathrm{H}},n_{\mathrm{H}})\,|^2 = 1+2\,\mathrm{Re}(U_{\mathrm{H}}(m_{\mathrm{H}},n_{\mathrm{H}}))+|\,U_{\mathrm{H}}(m_{\mathrm{H}},n_{\mathrm{H}})\,|^2, \quad (3)$$

where the first term is the direct current (DC) term, which represents the uniform wave field. It affects the reconstruction results slightly. The third term is the autocorrelation term. When the sample is relatively small and opaque, the term just has a minimal effect on the reconstruction.

The kernel of CS is the linear measurement process[8]. The theory verifies that accurate reconstruction can be obtained when the sufficient condition RIP is satisfied[14]. For a discrete 1D signal X whose length is N' and the number of nonzero elements is S ($S < N'$), the measured signal length is N' by conventional uniform sampling method. CS linear measurement process can measure the signal X with an $M'\times N'$ matrix Φ, and the observed value Y with a length of M' ($M' < N'$) is obtained. CS can realize the sparse representation of $X\times Y$, which usually equals solving the norm minimum problem. Likewise, CS is also applicable for the 2D and 3D signal processing. For a single hologram, the data volume is small compared with the required data for reconstructing a 3D structure, thus the hologram can be regarded as a sparse data. Moreover, the hologram is the linear recording of the sample diffraction field intensity, which satisfies the sparse conditions of CS. Therefore, CS can be used to reconstruct the 3D structure of the sample from a single hologram[9].

There is a linear mapping between the diffraction field and hologram I, which satisfies the linear measurement process. Then I is expressed as[9]

$$I = 2\,\mathrm{Re}\{Ho\} + e, \quad (4)$$

where H is the transformation matrix, e is the error effect of the DC and autocorrelation terms.

There is always a sharp contrast between the sample and background, thus the gradients of the image edge and high-frequency noise positions are large. The reconstruction plane is sparse by calculating total variation (TV) values[14]. The 3D reconstruction of the sample amplitude distribution can be conducted by solving the TV norm minimum based on CS theory. A sparsity restriction parameter is introduced to control the effect of TV values. Therefore, the answer to Eq. (3) is just the solution of minimizing the right terms of

$$o = \arg\min_{o\in \mathrm{R}}(||\,I-Ho\,||_2^2 + \tau\,||\,o\,||_{\mathrm{TV}}), \quad (5)$$

where τ is the sparsity restriction parameter,

$$\left\|o_k\right\|_{\mathrm{TV}} = \sum_{k=1}^{N_z}\sum_{m=1}^{N_1}\sum_{n=1}^{N_2}\left|\nabla(o_k(m,n))\right|.$$

The two-step iterative shrinkage/thresholding algorithm is used to solve Eq. (5)[12,15], which can be expressed as

$$o_1 = [o_0 + H'(I-Ho_0)/v] - 0.5\tau/v\left\|o_0 + H'(I-Ho_0)/v\right\|_{\mathrm{TV}}, \quad (6)$$

$$o_{t+1} = (1-a)o_{t-1} + (a-\beta)o_t + \beta\{[o_t + H'(I-Ho_t)/v] - 0.5\tau/v\left\|o_t + H'(I-Ho_t)/v\right\|_{\mathrm{TV}}\}$$
$$a = 2/\left(1+\sqrt{1-\left(\frac{1-\kappa}{1+\kappa}\right)^2}\right), \beta = 2a/(\lambda_1+\lambda_N), \kappa = \lambda_1/\lambda_N, \quad (7)$$

where λ_1 and λ_N represent the smallest and largest eigenvalues of the matrix H' H, respectively. In this letter, we define $\lambda_1 = 10^{-4}$, $\lambda_N = 1$ and v is the inverse scaling factor. The iteration can be ongoing by controlling the values of τ and $H'(I–Ho_t)$ terms. Iters is the total iteration number, $t = 1, 2...$, Iters. The initialization o_0 is set as a $N_1\times N_2\times N_z$ matrix whose elements are all one. It can be inferred from Eqs. (6) and (7) that the TV values of each iterative result have relatively large gradients at the image edge and high-frequency noise positions, and the others are zero or close to zero. After subtracting TV from the iterative results, filtering is realized. By choosing proper restriction parameter τ and iteration number Iters, the filtering degree can be controlled and the accurate reconstruction can also be realized.

Because the transparent area is far larger than the opaque sample in Gabor digital holography, most of the data in the recorded hologram are nonzero. By using the negative transformation the number of zero or close to zero values will be far more than that of nonzero. The hologram can be regarded as a sparse matrix, which accords with CS better than that without negative transformation. Then the hologram after processing is reconstructed with CS algorithm and the reconstructed image is inversed again. The image quality would be better in theory. Here the holograms in simulation and experiments are all processed this way when CS algorithm is used to reconstruct. The initial reconstruction plane is set at $z = 0$. The number of iterations of CS algorithm is 50 and the number of reconstruction planes is 2. Then the reconstructed images are normalized and piecewise-nonlinear transformation is conducted to enhance the image contrast. The piecewise-nonlinear transformation function is expressed as

$$g'(m,n) = \begin{cases} 0 & 0 \le g(m,n) \le a \\ g^{\gamma}(m,n) & a < g(m,n) \le b \\ 1 & b < g(m,n) \le 1 \end{cases}, \quad (8)$$

where $g(m, n)$ represents the value of the original image at (m, n), and g' is the result of transformation. The

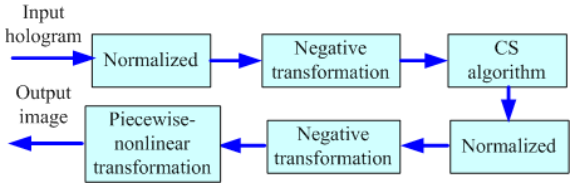

Fig. 2. Flow diagram of improved CS algorithm.

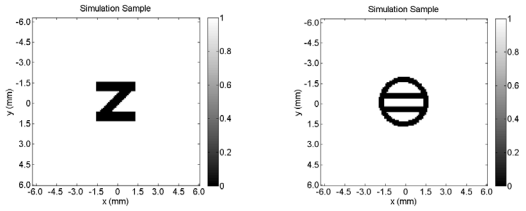

Fig. 3. Images of simulation samples.

exponent $\gamma < 1$ is a positive constant which controls the shape of the power-law transform curve.

The flow diagram of improved CS algorithm is shown in Fig. 2. The numerical simulation analysis of the reconstruction characteristics of the reconstruction algorithm has been conducted first. The pixel dimensions are set as 0.1×0.1 (mm) to correspond with the experiments. The number of pixels in a hologram is 124×124, and the wavelength is 118.83 μm. A "Z" letter whose dimensions are 2.9×2.9 (mm) and a ring with two horizontal lines in the center are used as the simulation samples. The widths of the horizontal and diagonal lines of "Z" are 0.7 and 0.6 mm, respectively. The diameter of the ring is 3.7 and the line width is 0.4 mm. The samples are shown in Fig. 3. Both samples are placed at 25 mm in the front of the detector. The ideal systematic lateral resolution is about 0.25 mm. The hologram is obtained based on Eq. (3) and a single hologram is used. The reconstruction results are shown in Figs. 4 and 5. The restriction parameter τ is 0.01.

The result (Figs. 4(b) and 5(b)) with CS algorithm suffers little from aperture diffraction and DC term effects. The outline is clear and the contrast is higher. The enhanced image is shown in Figs. 4(c) and 5(c). For the letter sample, the nonlinear transformation parameters (a, b, and γ) are 0.1, 0.9, and 0.4. For the ring sample, the nonlinear transformation parameters are 0.1, 0.85, and 0.4. It can be seen that image quality is further enhanced: the samples are separated from the background completely and have no background noise.

The CW 2.52 THz inline digital holographic imaging system in Ref. [7] is used. The pyroelectric camera (Pyrocam III, Ophir-Spiricon, Inc.) is used as the detector and has 124×124 pixels. The size of a pixel is 0.085×0.085 (mm), and the interval between pixels is 0.1×0.1 (mm). Firstly, a watch gear stuck to the transparent tape is measured. The diameter of the gear sample is 3.5 mm whose line width is about 0.3 mm. The

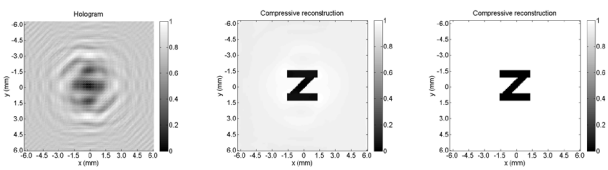

(a) (b) (c)

Fig. 4. Simulation "Z" sample's (a) hologram, (b) CS result, and (c) piecewise-nonlinear transformation result of (b).

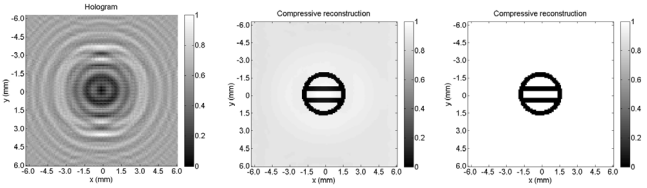

(a) (b) (c)

Fig. 5. Simulation result of ring sample: (a) hologram, (b) CS result, and (c) piecewise-nonlinear transformation result of (b).

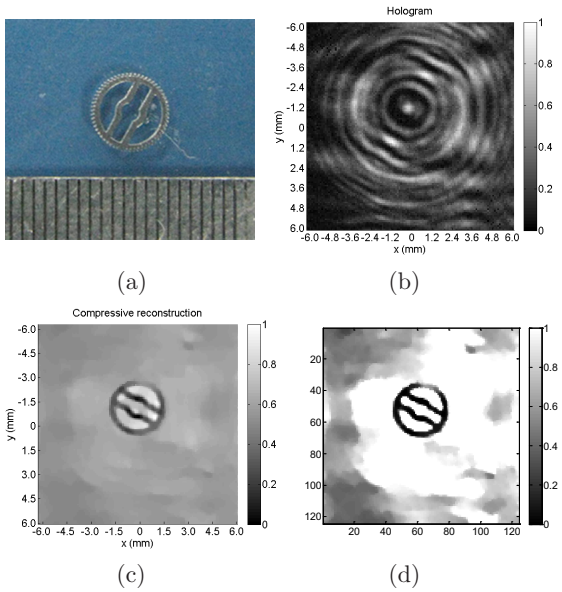

(a) (b) (c) (d)

Fig. 6. Reconstruction results of a watch gear: (a) photograph, (b) hologram, (c) CS result, and (d) piecewise-nonlinear transformation of (c).

sample is placed 19.6 mm away from the photosurface of the detector when the ideal resolution is about 0.2 mm. To improve the signal-to-noise ratio, the averaged holograms are 20 frames, respectively. The restriction parameter is 0.05. The photographs of the sample, holograms, and reconstructed images are shown in Fig. 6.

It can be seen that the images can reflect the sample structure characteristics mainly. However, the sawtooth structure of the gear is higher than the ideal resolution and cannot be accurately reconstructed. In addition, the image contrast is not sharp enough and the reconstructed image has a deficiency in the top-right corner. The possible reasons are that the transparent tape generates additional noise and the structure is very fine which lead to more obvious diffraction. Meanwhile, the sample surfaces are not parallel to the photosurface completely. The nonlinear transformation parameters are 0, 0.59, and 5. The image quality after image enhancement processing improves to a certain extent.

Then the handwritten "Z" letter sample on an A4 paper is measured and reconstructed. The dimensions of "Z" are nearly 3×2.8 (mm) whose line width is about 0.6 mm. The sample is placed about 46 mm away from the photosurface. Because the transmissivity

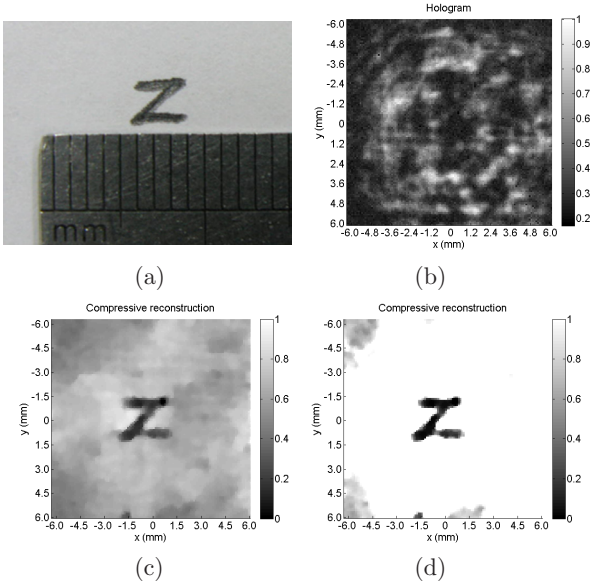

(a) (b) (c) (d)

Fig. 7. Reconstruction results of "Z" sample: (a) photograph, (b) hologram, (c) CS result, and (d) piecewise-nonlinear transformation of (c).

of the paper is low, the averaged holograms are all 80 frames. The restriction parameter is 0.01. The nonlinear transformation parameters are 0, 0.48, and 3. The results are shown in Fig. 7.

It can be seen that the reconstructed images can basically reflect the sample profiles. Because the contrast between the characters in pencil and paper is dull and the uniformity is also bad, the reconstruction results are not ideal. The "Z" sample is far away from the photosurface where the line width is close to the ideal resolution of about 0.45 mm, thus the strokes are thicker and the shape also changes.

In conclusion, detailed simulation and experimental studies demonstrate the feasibility of the algorithm in improving 2D reconstructed image quality in CW THz Gabor inline digital holography.

This work was supported by the National Natural Science Foundation of China (No. 61377110) and the Specialized Research Fund for the Doctoral Program of Higher Education of China (No. 20112302110028).

References

1. X. Gao, C. Li, and G. Y. Fang, Chin. Phys. Lett. **6,** 068401 (2011).
2. Q. Li, K. Xue, Y. D. Li, and Q. Wang, Appl. Opt. **51,** 7052 (2012).
3. M. S. Heimbeck, M. K. Kim, D. A. Gregory, and H. O. Everitt, Opt. Express **19,** 9192 (2011).
4. R. J. Mahon, J. A. Murphy, and W. Lanigan, Opt. Commun. **260,** 469 (2006).
5. Y. Zhang, W. Zhou, X. Wang, Y. Cui, and W. Sun, Strain **44,** 380 (2008).
6. I. McAuley, J. A. Murphy, N. Trappe, R. Mahon, D. McCarthy, and P. McLaughlin, Proc. SPIE **7939,** 1 (2011).
7. K. Xue, Q. Li, Y. D. Li, and Q. Wang, Opt. Lett. **37,** 3228 (2012).
8. D. L. Donoho, IEEE Trans. Inf. Theory **52,** 1289 (2006).
9. D. J. Brady, K. Choi, D. L. Marks, R. Horisaki, and S. Lim, Opt. Express **17,** 13040 (2009).
10. C. F. Cull, D. A. Wikner, J. N. Mait, M. Mattheiss, and D. J. Brady, Appl. Opt. **49,** E67 (2010).
11. S. Lim, D. L. Marks, and D. J. Brady, Appl. Opt. **50,** H75 (2011).
12. L. Denis, D. Lorenz, E. Thiébaut, C. Fournier, and D. Trade, Opt. Lett. **34,** 3475 (2009).
13. Q. Li and Y. D. Li, Appl. Phys. B **117,** 586 (2014).
14. E. Candes, J. Romberg, and T. Tao, IEEE Trans. Inf. Theory **52,** 489 (2006).
15. J. M. Bioucas-Das and M. A. T. Figueiredo, IEEE Trans. Image Process. **16,** 2992 (2007).